Synergistic active and passive shimming to optimize B_0 field homogeneity in micro MR imaging

R. Dewal[1], Z. Cao[1], C. Sica[2], C. Collins[2], and Q. Yang[1,2]

[1]Bioengineering, The Pennsylvania State University, Hershey, PA, United States, [2]Radiology, The Pennsylvania State University, Hershey, PA, United States

Introduction: The active shimming methods developed for NMR spectroscopy in a uniform sample are known to be less effective for high field *in vivo* MR imaging studies because of the local higher-order gradients in regions near air-tissue interfaces, such as the paranasal sinuses and ear canals. Attempts have been made to address this issue with a passive shimming approach, but there are requirements that make implementation for general use difficult [1]. Here, we present a synergistic shimming algorithm that simultaneously optimizes the linear active shim coil settings and the higher-order local passive shimming configurations for a specific sample. This approach is expected to be applicable to standard high-field MRI systems for both animal and human studies.

Methods: The optimization method is comprised of two steps as shown in Figure 1: (1) a fast, but approximate analytical solution-based calculation and (2) a slower, but more accurate numerical Fourier Transform-based calculation. Eight cylinders of fixed diameter (6.35 mm) and variable position, length, and susceptibility were used as the shim elements. First, these shim elements were scattered around the sample. The effects of the shim elements on B_0 were then approximated using the analytical solution for the perturbation field of a sphere of homogeneous material with a given susceptibility and linearly superimposed with the B_0 field in the sample [2]. The optimal first-order active shim values were calculated using the Moore-Penrose pseudo-inverse [3]. The suitability of the shim setup was then evaluated by calculating the variance of the shimmed ΔB_0 field within the volume of interest (VOI). The locations, lengths, and susceptibility values of the cylinders were then iteratively optimized by using a constrained numerical minimization function until a stopping criterion was reached. The solution output from this round of optimization was then used as the starting point for the next round of optimization, which used a Fourier transform-based method to calculate the B_0 field perturbation of the shim cylinders instead of the analytical solution [4]. All simulation experiments were performed in MATLAB (The MathWorks, Inc., Natick, MA) on a 256x256x256 matrix, 0.5 mm voxel size 2% agar gel phantom model as shown in Figure 2.

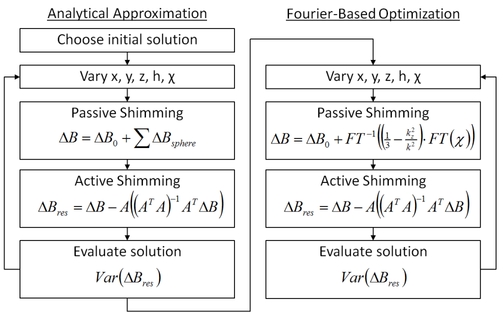

Figure 1. Workflow of the iterative optimization method.

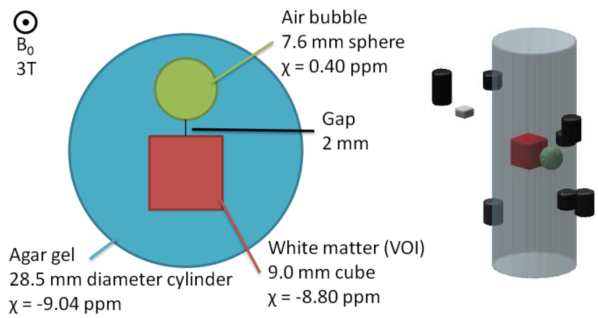

Figure 2. (Left) A cross-sectional diagram of the computer agar gel model. (Right) A stylized 3D rendering of the cylindrical agar gel phantom and optimized shim pieces.

Results: Figure 2 shows the optimized configuration of the shim elements with respect to the phantom. Figure 3 shows ΔB_0 maps of slices through the center of the model with active shimming (left) and synergistic shimming (right). With linear active shimming alone, the B_0 field in the cubical VOI remained highly inhomogeneous. Our algorithm was able to find simultaneous configurations of linear active shims and passive shim elements that markedly reduced the overall B_0 inhomogeneity in the VOI with a 3-fold reduction in ΔB_0 variance within the VOI.

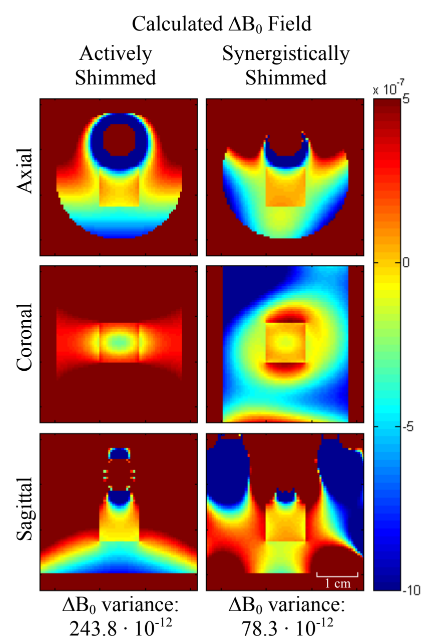

Figure 3. Synergistic shimming results in markedly reduced B_0 field inhomogeneity as compared to active shimming alone.

Discussion: Using simulations of an inhomogeneous sample, we have illustrated the potential to significantly improve B_0 homogeneity over conventional active shimming alone with synergistic use of active and passive shimming. In practice, this should allow for more effective artifact reduction in brain regions near air-tissue interfaces. Though these results are entirely in simulation, the methodology and computer software are geared towards real-time shimming for *in vivo* studies. The choice of cylindrical shim pieces of fixed diameter was made with experimental implementation in mind. The susceptibility values of the shim materials were also chosen such that they are commercially available. The materials that are under consideration are bismuth, zirconium, titanium, and niobium. This was taken into account in the optimization routine by properly setting the bounds on the shim susceptibility values in the MATLAB solver.

The algorithm makes some simplifying assumptions. The perturbations to the B_0 field from the shim elements and from the subject are assumed to add linearly; due to the large difference in susceptibility value between the shim elements and the subject tissue, this should not and does not appear to affect results significantly. In the case of the analytical approximation, the cylinders are approximated using spheres of equal volume, and perturbations from each sphere are added to the B_0 field via linear superposition. This latter assumption holds to some extent far away from the shim elements [1]. However, some shim elements are necessarily close to the target tissue, rendering this a rough approximation. Therefore, the nimble analytical approximation is best used to provide an acceptable starting point for the slower, but more accurate Fourier transform-based optimization. Future work includes using a global optimization procedure in conjunction with the analytical approximation in order to provide an even better shimming solution while keeping the time taken by the method low enough to be practical for real-time application *in vivo*.

Acknowledgments: Funding has been provided in part through NIH R01 AG027771, NIH R01 EB000454, and the Pennsylvania Department of Health.

References:

[1] Koch et al. J Magn Reson 182 (2006) 66–74
[2] Schenck, John. Med Phys 23 (6) (1996) 815-850
[3] Cao et al., Proc. ISMRM 2010, p. 1544
[4] Salomir et al. Concepts Magn Reson Part B (Magn Reson Engineering) 19B (2003) 26–34